J Therm Anal Calorim (2013) 113:609–613
DOI 10.1007/s10973-012-2723-6

Magnetocaloric properties of $La_{0.6}Ca_{0.4}MnO_3$

Mahmoud Aly Hamad

Received: 20 May 2012 / Accepted: 21 September 2012 / Published online: 21 October 2012

Abstract A theoretic work on magnetocaloric properties of the polycrystalline $La_{0.6}Ca_{0.4}MnO_3$ system near a second-order phase transition from a ferromagnetic to a paramagnetic state is presented. The value of the magnetocaloric effect has been determined from the calculation of magnetization as a function of temperature under different external magnetic field shifts. The magnetic entropy change ΔS_M reaches a peak of about 3 J kg^{-1} K^{-1} at 266 K upon 1.60 KA/m applied field variation. The ΔS_M distribution is much more uniform than that of gadolinium, which is desirable for an Ericson-cycle magnetic refrigerator, which is beneficial for the household application of active magnetic refrigerant materials.

Keywords $La_{0.6}Ca_{0.4}MnO_3$ · Magnetocaloric effect · Model · Magnetic entropy change · Heat capacity change

Introduction

The refrigeration by magnetocaloric effect (MCE) and electrocaloric effect (ECE) offer a lot of clear advantages over the conventional gas compression refrigeration technology [1–9]. These provide efficient and environment-friendly solutions for cooling. It is more efficient, inexpensive, and environmentally friendly for replacing the current refrigerators using greenhouse gases that are harmful to environment and contributing to global warming.

Characterization and application of the magnetic properties of ferromagnetic particles become increasingly important for the level of miniaturization and reliability necessary for commercialization [10].

Perovskite manganites have attracted significant attention since the discovery of colossal magnetoresistance and several interesting properties of these compounds have been found. In recently years, there has been an increasing interest in using manganites not only as a material having colossal magnetoresistivity but also as a material with interesting magnetocaloric properties [11–13].

A large magnetocaloric effect makes manganites excellent candidates for working materials in magnetic refrigeration units especially because they are less costly than other materials, particularly those based on Gd.

In this paper, theoretic work on magnetization versus temperature in different magnetic field shifts for polycrystalline $La_{0.6}Ca_{0.4}MnO_3$ system. It is used a phenomenological model for simulation of magnetization dependence on temperature variation to predict magnetocaloric properties such as magnetic entropy change, heat capacity change, temperature change, and relative cooling power.

Theoretic considerations

According to phenomenological model in Hamad [14], the dependence of magnetization on variation of temperature and Curie temperature T_c is presented by

$$M = \left(\frac{M_i - M_f}{2}\right)[\tanh(A(T_C - T))] + BT + C, \quad (1)$$

where M_i is an initial value of magnetization at ferromagnetic–paramagnetic transition and M_f is a final value of magnetization at ferromagnetic–paramagnetic transition as shown in Fig. 1.

M. A. Hamad (✉)
Department of Physics, College of Science, Al-Jouf University, P.O. Box 2014, Skaka, Al-Jouf, Saudi Arabia
e-mail: m_hamad76@yahoo.com

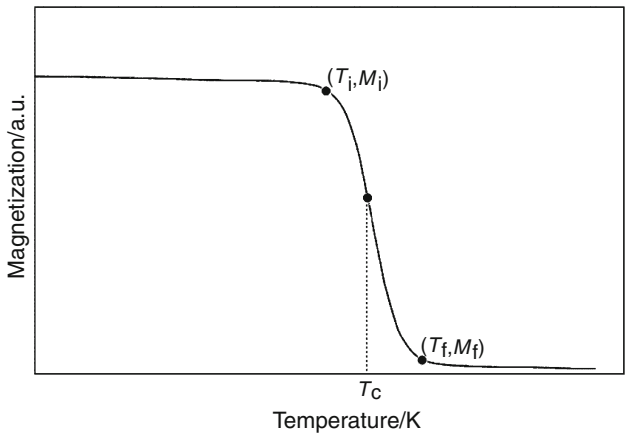

Fig. 1 Temperature dependence of magnetization in constant applied field

$$A = \frac{2(B - S_c)}{M_i - M_f},$$

B is magnetization sensitivity $\frac{dM}{dT}$ at ferromagnetic state before transition, S_c is magnetization sensitivity $\frac{dM}{dT}$ at Curie temperature T_C and

$$C = \left(\frac{M_i + M_f}{2}\right) - BT_C.$$

A magnetic entropy change of a magnetic system under adiabatic magnetic field variation from 0 to final value H_{max} is available by

$$\Delta S_M = \left(-A\left(\frac{M_i - M_f}{2}\right)\text{sech}^2(A(T_C - T)) + B\right)H_{Max}. \tag{2}$$

The foundation of large magnetic entropy change is attributed to high magnetic moment and rapid change of magnetization at T_c. A result of Eq. (2) is a maximum magnetic entropy change ΔS_{Max} (where $T = T_C$) can be evaluated as following the equation

$$\Delta S_{Max} = H_{Max}\left(-A\left(\frac{M_i - M_f}{2}\right) + B\right). \tag{3}$$

Eq. (3) is an important equation for taking into consideration of value of the magnetic entropy change to evaluate magnetic cooling efficiency with its full-width at half-maximum.

A determination of full-width at half-maximum(δT_{FWHM}) can be evaluated as follows:

$$\delta T_{FWHM} = \frac{2}{A}\cosh^{-1}\left(\sqrt{\frac{2A(M_i - M_f)}{A(M_i - M_f) + 2B}}\right). \tag{4}$$

This equation gives a full-width at half-maximum magnetic entropy change contributing for estimation of magnetic cooling efficiency as follows.

A magnetic cooling efficiency is estimated by considering magnitude of magnetic entropy change, ΔS_M and its full-width at half-maximum (δT_{FWHM}) [13]. A product of $-\Delta S_{Max}$ and δT_{FWHM} is called relative cooling power (RCP) based on magnetic entropy change.

$$\begin{aligned} RCP &= -\Delta S_M(T, H_{Max}) \times \delta T_{FWHM} \\ &= \left(M_i - M_f - 2\frac{B}{A}\right)H_{Max} \\ &\quad \times \cosh^{-1}\left(\sqrt{\frac{2A(M_i - M_f)}{A(M_i - M_f) + 2B}}\right). \end{aligned} \tag{5}$$

The magnetization-related change of the specific heat is given by [13]

$$\Delta C_{P,H} = T\frac{\delta\,\Delta S_M}{\delta T}. \tag{6}$$

According this model [14], $\Delta C_{P,H}$ can be rewritten as

$$\begin{aligned} \Delta C_{P,H} = &-TA^2(M_i - M_f)\ \text{sech}^2(A(T_C - T)) \\ &\tanh(A(T_C - T))H_{Max}. \end{aligned} \tag{7}$$

A temperature change of a magnetic system under adiabatic magnetic field variation from 0 to H_{max} can be written in the form

$$\begin{aligned} \Delta T &= -\frac{T}{C_P}\int_0^{H_{Max}}\left(\frac{\partial M}{\partial T}\right)_E dH, \\ &= \frac{AT(M_i - M_f)}{2C_P}\left[\text{sech}^2(A(T_C - T)) + B\right]H_{Max}. \end{aligned} \tag{8}$$

C_p is the heat capacity per mole at constant magnetic field.

Table 1 Model parameters for $La_{0.6}Ca_{0.4}MnO_3$ in different applied magnetic fields

H/KA m^{-1}	M_i/A m^2 kg^{-1}	M_f/A m^2 kg^{-1}	T_c/K	B/A m^2 kg^{-1} K^{-1}	S_c/A m^2 kg^{-1} K^{-1}
0.08	51.25	3.65	253	−0.11	−4.08
0.16	56.30	7.00	255	−0.29	−3.22
0.40	59.50	8.50	257	−0.23	−2.45
0.80	59.80	11.00	261	−0.24	−1.91
1.60	60.10	17.10	266	−0.23	−1.50

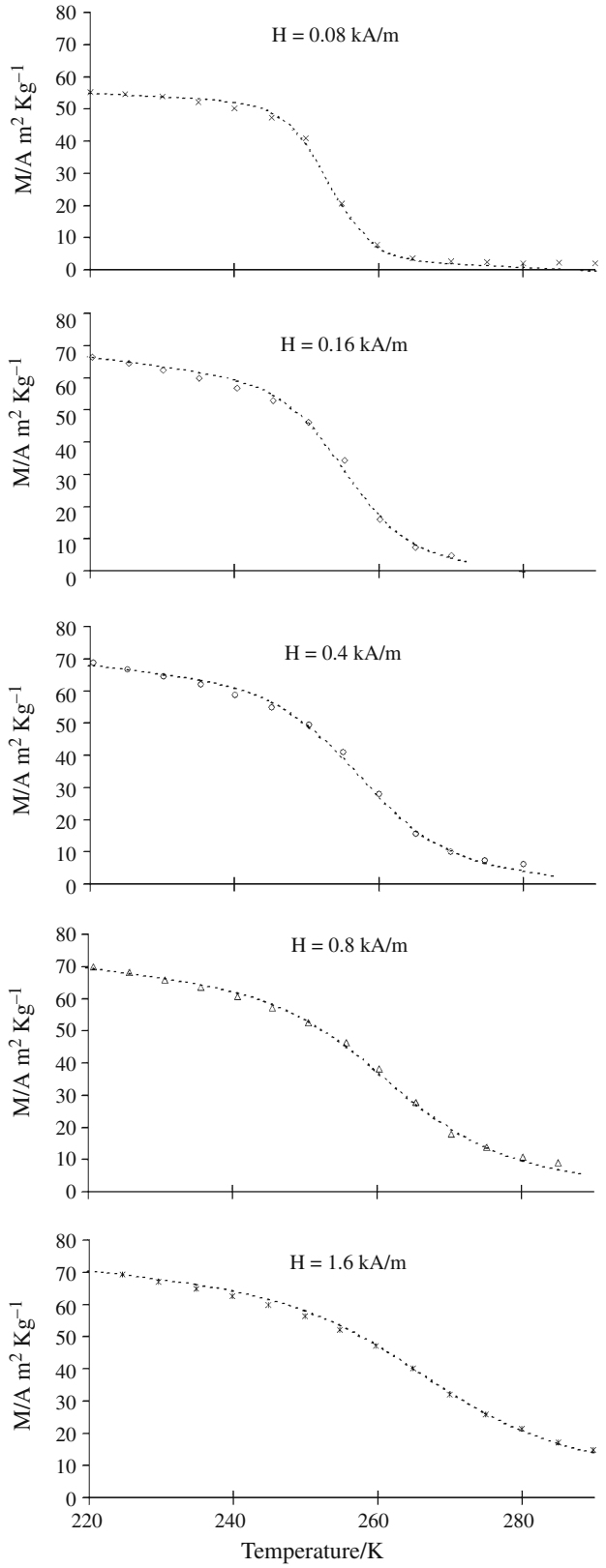

Fig. 2 Magnetization in different applied magnetic field shifts for the $La_{0.6}Ca_{0.4}MnO_3$ versus temperature. The *dashed curves* are modeled results and symbols represent experimental data from ref. [12]

From this phenomenological model, it can easily assess the values of δT_{FWHM}, $|\Delta S|_{max}$, RCP, and ΔT for $La_{0.6}Ca_{0.4}MnO_3$ under magnetic field variation.

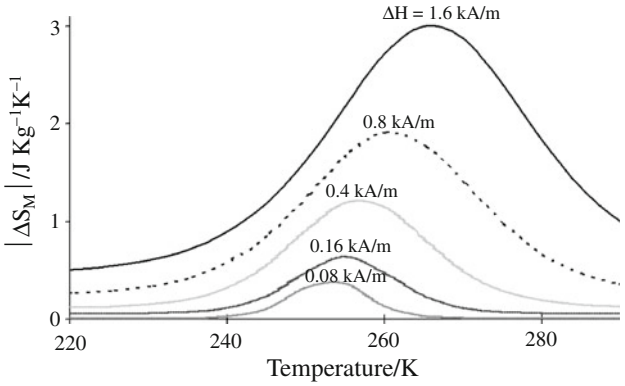

Fig. 3 Magnetic entropy change as function of temperature for $La_{0.6}Ca_{0.4}MnO_3$ in different applied magnetic field shifts

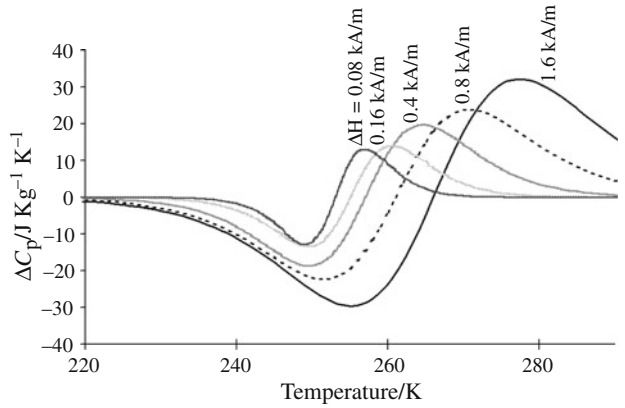

Fig. 4 Heat capacity changes as function of temperature for $La_{0.6}Ca_{0.4}MnO_3$ in different applied magnetic field shifts

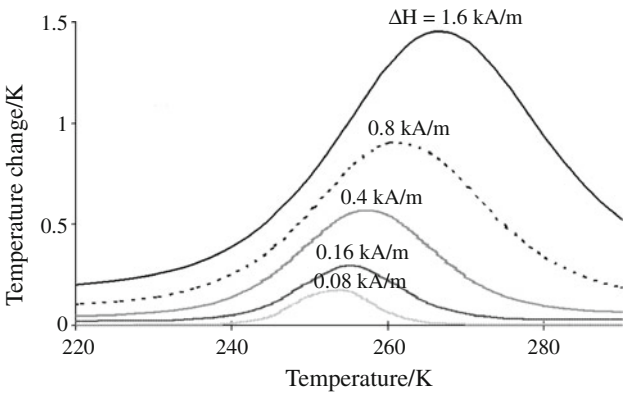

Fig. 5 Temperature changes as function of temperature for $La_{0.6}Ca_{0.4}MnO_3$ in different applied magnetic field shifts

Table 2 The predicted values of applied magnetocaloric properties for $La_{0.6}Ca_{0.4}MnO_3$ in different applied magnetic field shifts

ΔH/KA m^{-1}	$-\Delta S_{max}$/J kg^{-1} K^{-1}	δT_{FWHM}/K	RCP/J kg^{-1}	$\Delta C_{P,H(max)}$/J kg^{-1} K^{-1}	$\Delta C_{P,H(min)}$/J kg^{-1} K^{-1}	$\lvert\Delta T\rvert_{max}$/K
0.08	0.37	10.80	4.024	13.16	−12.75	0.17
0.16	0.65	16.04	10.37	13.98	−13.35	0.30
0.40	1.20	21.98	26.33	19.75	−18.59	0.56
0.80	1.92	28.85	55.26	23.93	−22.20	0.91
1.60	3.00	34.42	103.39	32.14	−29.59	1.45

Theoretic work

Numerical calculations were made with parameters as displayed in Table 1. A heat capacity $C_p = 550$ J kg^{-1} K^{-1} [15, 16]. Figure 2 shows the magnetization versus temperature in different applied magnetic field shifts for $La_{0.6}Ca_{0.4}MnO_3$ polycrystals have been prepared by a non-standard ceramic method with presintering at 1,100 °C and final sintering at 1,350 °C. The symbols represent experimental data from ref. [12], while the dashed curves represent modeled data using model parameters given in Table 1. It is seen that for the given parameters, the results of calculation are in a good agreement with the experimental results. Furthermore, Figs. 3, 4, and 5 show predicted values for changes of magnetic entropy, specific heat, and temperature versus temperature. Magnetic entropy change in $La_{0.6}Ca_{0.4}MnO_3$ is reported in Fig. 3 and shows an increase in $|\Delta S_M|$ with increasing ΔH. The magnetic entropy change curves reveal the characteristics of the spin reorientation by the kinks in the ΔS_M curve. The maxima observed in the ΔS_M curves are associated to a spin reorientation that occurs continuously. The behavior of curves suggests how to extend the range of temperatures for use in the MCE.

The values of maximum magnetic entropy change, full-width at half-maximum, and relative cooling power at different magnetic field shifts for $La_{0.6}Ca_{0.4}MnO_3$ are calculated by Eqs. 3–5, respectively, and tabulated in Table 2. Furthermore, the maximum and minimum values of specific heat change for each sample is determined from Fig. 4.

Both ΔS_M and ΔT reflect a fundamental importance on the understanding of the behavior of the MCE, and these terms can be approximately estimated by Eqs. 2 and 8, respectively. As shown in Fig. 3, ΔS_M reaches a peak of about 3 J kg^{-1} K^{-1} at 266 K upon 1.60 KA/m applied field variation. Though the maximum ΔS_M is 1.92 J kg^{-1} K^{-1} upon 0.80 KA/m applied field variation which is about 70 % of that of a pure Gd metal 2.8 J kg^{-1} K^{-1} upon 0.80 KA/m, the ΔS_M distribution of the $La_{0.6}Ca_{0.4}MnO_3$ is much more uniform than that of gadolinium [17, 18]. This feature is desirable for an Ericsson-cycle magnetic refrigerator [19].

Although $La_{0.6}Ca_{0.4}MnO_3$ is very similarly to research $La_{0.67}Ca_{0.33}MnO_3$ in Hamad [14], the magnetic entropy changes of $La_{0.6}Ca_{0.4}MnO_3$ and $La_{0.67}Ca_{0.33}MnO_3$ have great difference. This due to the methods and conditions of synthesizing of two samples are different. Moreover, the former has a polycrystalline structure, while the latter has a single crystalline structure.

In general, the large magnetic entropy change in perovskite manganites has been believed to be related to the considerable variation of magnetization near T_C [20]. The spin–lattice coupling in the magnetic ordering process could play a significant role in additional magnetic entropy change [21]. Owing to the strong coupling between spin and lattice, significant lattice change accompanying magnetic transition in perovskite manganites has been observed [22, 23]. The lattice structural change in the Mn–O bond distance as well as Mn–O–Mn bond angle would, in turn, favor the spin ordering. Thereby, a more abrupt reduction of magnetization near T_C occurs and results in a significant magnetic entropy change [16, 24–26]. In this way, a conclusion might be drawn that a strong spin–lattice coupling in the magnetic transition process would lead to additional magnetic entropy change near T_C, and consequently, favors the MCE.

Conclusions

Dependence of the magnetization on temperature variation for $La_{0.6}Ca_{0.4}MnO_3$ upon different magnetic fields was simulated. In general, this allows the prediction of magnetocaloric properties of $La_{0.6}Ca_{0.4}MnO_3$ such as magnetic entropy change, full-width at half-maximum, relative cooling power, and magnetic specific heat change for $La_{0.6}Ca_{0.4}MnO_3$ upon different magnetic field shifts. Though the maximum ΔS_M is about 70 % of that of gadolinium, the ΔS_M distribution is much more uniform than that of gadolinium, which is desirable for an Ericsson-cycle magnetic refrigerator, which is beneficial for the household application of active magnetic refrigerant materials.

References

1. Oliveira NA, Ranke PJ. Theoretical aspects of the magnetocaloric effect. Phys Rep. 2010;489:89.
2. Gschneidner KA, Pecharsky VK, Tsoko AO. Recent developments in magnetocaloric materials. Rep Prog Phys. 2005;68:1479–539.

3. Szymczak R, Czepelak M, Kolano R, Burian AK, Krzymanska B, Szymczak H. Magnetocaloric effect in $La_{1-x}Ca_xMnO_3$ for x = 0.3, 0.35, and 0.4. J Mater Sci. 2008;43:1734–9.
4. Hamad MA. Magneto-caloric effect in Ge0.95Mn0.05 films. J Supercond Nov Magn. 2012. doi:10.1007/s10948-012-1762-3.
5. Hamad MA. Magnetocaloric effect in polycrystalline $Gd_{1-x}Ca_x$-$BaCo_2O_{5.5}$. Mater Lett. 2012;82:181–3.
6. Hamad MA. Calculation on electrocaloric properties of ferroelectric $SrBi_2Ta_2O_9$. Ph Transitions. 2012;85:159–68.
7. Hamad MA. Investigations on electrocaloric properties of [111]-oriented $0.955PbZn_{1/3}Nb_{2/3}O_3$–$0.045PbTiO_3$ single crystals. Ph Transitions. 2012. doi:10.1080/01411594.2012.674527.
8. Hamad MA. Detecting giant electrocaloric effect in $Sr_xBa_{1-x}Nb_2O_6$ single crystals. Appl Phys Lett. 2012;100:192908.
9. Hamad MA. Theoretical investigations on electrocaloric properties of relaxor ferroelectric $0.9PbMg_{1/3}Nb_{2/3}O_3$-$0.1PbTiO_3$ thin film. J Comput Electron. 2012. doi:10.1007/s10825-012-0414-y.
10. Hamad MA. Prediction of energy loss of $Ni_{0.58}Zn_{0.42}Fe_2O_4$ nanocrystalline and Fe_3O_4 nanowire arrays. Jpn J Appl Phys. 2010;49:085004.
11. Banerjee S, Kumar A, Devi PS. Preparation of nanoparticles of oxides by the citrate–nitrate process. J Therm Anal Calorim. 2011;104:859–67.
12. Szymczak R, Czepelak M, Kolano R, Burian AK, Krzymanska B, Szymczak H. Magnetocaloric effect in $La_{1-x}Ca_xMnO_3$ for x = 0.3, 0.35, and 0.4. J Mater Sci. 2008; 43:1734–1739.
13. Hamad MA. Theoretical work on magnetocaloric effect in ceramic and sol-gel La0.67Ca0.33MnO3. J Therm Anal Calorim. 2012. doi:10.1007/s10973-012-2505-1.
14. Hamad MA. Prediction of thermomagnetic properties of $La_{0.67}Ca_{0.33}MnO_3$ and $La_{0.67}Sr_{0.33}MnO_3$. Ph Transitions. 2012;85:106–12.
15. Kumar N, Kishan H, Rao A, Awana VPS. Structural, electrical, magnetic, and thermal studies of Cr-doped $La_{0.7}Ca_{0.3}Mn_{1-x}Cr_xO_3$ ($0 \leq x \leq 1$) manganites. J Appl Phys. 2010;107:083905.
16. Bohigas X, Tejada J, Sarrion MLM, Tripp S, Black R. Magnetic and calorimetric measurements on the magnetocaloric effect in $La_{0.6}Ca_{0.4}MnO_3$. J Magn Magn Mater. 2000;208(1–2):85–92.
17. Goodenough JB. Theory of the role of covalence in the perovskite-type manganites [La, M(II)]MnO_3. Phys Rev. 1955;100:564.
18. Dan'kov SY, Tishin AM, Pecharsky VK, Gschneidner KA. Magnetic phase transitions and the magnetothermal properties of gadolinium. Phys Rev B. 1998;57:3478.
19. Pecharsky VK, Gschneidner KA. Magnetocaloric effect and magnetic refrigeration. J Magn Magn Mater. 1999;200:44–56.
20. Bohigas X, Tejada J, Barco E, Zhang XX, Sales M. Tunable magnetocaloric effect in ceramic perovskites. Appl Phys Lett. 1998;73:390.
21. Guo ZB, Du YW, Zhu JS, Huang H, Ding WP, Feng D. Large magnetic entropy change in perovskite-type manganese oxides. Phys Rev Lett. 1997;78:1142.
22. Radaelli PG, Cox DE, Marezio M, Cheong SW, Schiffer PE, Ramirez AP. Simultaneous structural, magnetic, and electronic transitions in $La_{1-x}Ca_xMnO_3$ with x = 0.25 and 0.50. Phys Rev Lett. 1995;75:4488.
23. Kim KH, GU JY, Choi HS, Park GW, Noh TW. Frequency shifts of the internal phonon modes in La0.7Ca0.3MnO3. Phys Rev Lett. 1996;77:1877.
24. Tang T, Gu KM, Cao QQ, Wang DH, Zhang SY, Du YW. Magnetocaloric properties of Ag-substituted perovskite-type manganites. J Magn Magn Mater. 2000;222:110–4.
25. Phan MH, Yu SC. Review of the magnetocaloric effect in manganite materials. J Magn Magn Mater. 2007;308:325–40.
26. Sun Y, Tong W, Zhang YH. Large magnetic entropy change above 300 K in La0.67Sr0.33Mn0.9Cr0.1O3. J Magn Magn Mater. 2001;232:205–8.